

DISCOVERY OF GEV EMISSION FROM THE DIRECTION OF THE LUMINOUS INFRARED GALAXY NGC 2146

QING-WEN TANG^{1,2}, XIANG-YU WANG^{1,2} AND PAK-HIN THOMAS TAM³

¹ School of Astronomy and Space Science, Nanjing University, Nanjing, 210093, China;
xywang@nju.edu.cn

² Key laboratory of Modern Astronomy and Astrophysics (Nanjing University), Ministry of Education, Nanjing 210093, China

³ Institute of Astronomy and Department of Physics, National Tsing Hua University, Hsinchu 30013, Taiwan
phtam@phys.nthu.edu.tw

Draft version August 11, 2014

ABSTRACT

Recent detection of high-energy gamma-ray emission from starburst galaxies M82 and NGC 253 suggests that starburst galaxies are huge reservoirs of cosmic rays and these cosmic rays convert a significant fraction of their energy into gamma-rays by colliding with the dense interstellar medium. In this paper, we report the search for high-energy gamma-ray emission from several nearby star-forming and starburst galaxies using the 68 month data obtained with the Fermi Large Area Telescope. We found a $\sim 5.5\sigma$ detection of gamma-ray emission above 200MeV from a source spatially coincident with the location of the luminous infrared galaxy NGC 2146. Taking into account also the temporal and spectral properties of the gamma-ray emission, we suggest that the gamma-ray source is likely to be the counterpart of NGC 2146. The gamma-ray luminosity suggests that cosmic rays in NGC 2146 convert most of their energy into secondary pions, so NGC 2146 is a "proton calorimeter". It is also found that NGC 2146 obeys the quasi-linear scaling relation between the gamma-ray luminosity and total infrared luminosity for star-forming galaxies, strengthening the connection between massive star formation and gamma-ray emission of star-forming galaxies. Possible TeV emission from NGC 2146 is predicted and the implications for high-energy neutrino emission from starburst galaxies are discussed.

Subject headings: cosmic rays — galaxies: starburst

1. INTRODUCTION

It is generally believed that Galactic cosmic rays (CR) are accelerated by supernova remnant (SNRs) shocks (Ginzburg & Syrovatskii 1964). CR protons interact with the interstellar gas and produce neutral pions (schematically written as $p + p \rightarrow \pi^0 + \text{other products}$), which in turn decay into gamma-rays ($\pi^0 \rightarrow \gamma + \gamma$). The high SN rate in starburst galaxies implies high CR emissivities, so they are predicted to be bright gamma-ray sources (e.g. Domingo-Santamaría & Torres (2005); Rephaeli et al. (2010); Lacki et al. (2010); Ackermann et al. (2012)). The gamma-ray luminosity of starbursts depends not only on the CR intensity, but also on the conversion efficiency of CR proton energy into pionic gamma-rays. This efficiency in turn depends on the ratio of the timescale of pion production to the escape time of protons. Protons escape by advection in galactic winds or by diffusion. A galaxy becomes a "proton calorimeter" when the pion production time is shorter than the escape time, i.e. CR protons lose almost all of their energy to pionic collisions before escaping (Thompson et al. 2007). The detection of high-energy gamma-ray emission from starburst galaxies M82 and NGC 253 suggest that CR protons convert a significant fraction of their energy into secondary pions (Abdo et al. 2010a), so they are close to be "proton calorimeter" (Lacki et al. 2011).

Ackermann et al. (2012) (hereafter ACK12) examined a sample of 64 dwarf, spiral, and luminous and ultra-luminous infrared galaxies using 3 years of data collected by the Large Area Telescope (LAT) on the Fermi Gamma-ray Space Telescope. With a larger sample of significantly detected sources and flux upper limits for the remaining galaxies, they found that the gamma-ray luminosity and total infrared luminosity of star-forming galaxies are correlated. The obtained scaling

relations allow straightforward predictions for the next star-forming galaxies that could be detected by Fermi/LAT. Seven galaxies are selected by ACK12 as the best candidates with the highest probabilities for the next Fermi/LAT detection beyond the Local Group: M83, NGC 3690, NGC 2146, Arp 220, NGC 1365, M51, and M101.

We search for high-energy gamma-ray emission from the above 7 galaxies using the 68 month Fermi/LAT data. We found significant detection of gamma-ray emission from NGC 2146, the nearest luminous infrared galaxies (LIRGs). LIRGs are extreme starburst galaxies with total infrared luminosity in $8\text{--}1000\ \mu\text{m} \gtrsim 10^{11} L_{\odot}$ (Sanders & Mirabel 1996). They have very high star formation rate (SFR) in concentrated regions. The high infrared luminosities are due to large amounts of dust, which absorb ultra-violet (UV) photons and re-radiate them in the infrared (IR). NGC 2146 has $L_{8\text{--}1000\mu\text{m}} \simeq 10^{11} L_{\odot}$ at distance of $D = 15.2\text{Mpc}$ (Gao & Solomon 2004). For the other 6 galaxies, upper limits on the gamma-ray flux are obtained.

2. LAT DATA ANALYSIS AND RESULTS

2.1. Data reduction and analysis

Our sample comprises 7 star-forming galaxies which are selected by ACK12 as the most promising sources for Fermi/LAT detection. Here we present the data derived from the Fermi/LAT observations from 2008 August 4(MJD 54, 682) to 2014 April 4(MJD 56,752). Photons with energy between 200MeV and 100 GeV are selected to be analyzed when using the Fermi Science Tools package, version v9r32p5. Instrument response functions(IRFS) of P7REP_SOURCE_V15 is used for these events of source class. Also, we excluded the events with zenith angles $>100^\circ$ in order to avoid a significant contribution of Earth-limb

gamma-rays. All events in a region of interest (ROI) of 10° around the positions of galaxies have been used, and all sources within 15° listed in the second Fermi catalog (Nolan et al. 2012) (2FGL catalog) were modeled to produce the spectra and calculate the test statistic (TS, see e.g., Mattox et al. (1996)) of the source. The diffuse Galactic and extragalactic background components were modeled with the files `gll_iem_v05.fits` and `iso_source_v05.txt`, respectively. All galaxies were modeled with a power law spectra $N(E) = N_0(E/E_0)^{-\Gamma}$, where Γ is the photon index. To assess the detection significance of gamma-ray emission for galaxies, unbinned likelihood analysis are performed with the model described above. If the corresponding TS value is above 25, we derived the best-fit position using the tool *gtfindsrc*. For the sources included in the 2FGL catalog, we fixed their position to the values from the catalog. Then we perform the maximum likelihood analysis again to refine the spectral parameters of the sources within the ROI and the diffuse sources using the *gtlike*. Binned likelihood analysis was also performed to verify the results.

2.2. NGC 2146

A significant gamma-ray excess with TS of 30.8 (corresponding to a detection significance $\approx 5.5\sigma$) was found at the best-fit gamma-ray position (R.A., Decl.)=(94.55°, 78.30°). This position is consistent with the core of NGC 2146, the nearest LIRG galaxy. Detection significance map for NGC 2146 is shown in Fig. 1. This result unambiguously confirms an earlier, marginally significant excess (TS \sim 20) in the direction of NGC 2146 reported in ACK12. The 0.2-100 GeV spectrum of NGC 2146 is best described by a power law with $\Gamma=2.1\pm 0.2$ and a photon flux of $F(0.2-100\text{GeV})=(1.1\pm 0.5)\times 10^{-9}\text{ cm}^{-2}\text{s}^{-1}$. The localization and spectral results of the likelihood analysis are summarized in Table 1. We also performed an additional maximum likelihood analysis by dividing the energy range 0.2–100 GeV into six energy bins, and the spectrum is shown in Fig. 2.

We test alternative associations for the gamma-ray excess besides NGC 2146 in the CRATES catalog (Healey et al. 2007) of flat-spectrum radio sources (FSRQs), Veron-Cetty Catalog of Quasars & AGN (Véron-Cetty & Véron 2010) and the Candidate Gamma-Ray Blazar Survey catalog, CGRaBS (Healey et al. 2008). In the vicinity of NGC 2146, the only possible gamma-ray emitting object is the FSRQ CRATES J061758+781552 (also named CGRaBS J0617+7816 with redshift of 1.43 (Caccianiga et al. 2000)), which is 0.04° away from best-fit gamma-ray position.

We searched for gamma-ray flux variability by creating a 7-month-per-bin light curve of the photon flux > 400 MeV arriving from within a circular region of 10° in radius centered on the best-fit gamma-ray position, which is shown in Fig. 2. Measuring the goodness-of-fit of the light curve using the average flux over the years gives a reduced χ^2 of 0.84 with 7 degrees of freedom, while upper limits were not included. Lack of variability is consistent with a starburst galaxy origin, while FSRQs with such a low variability in gamma-rays is rare among LAT blazars. The photon index -2.1 ± 0.2 also agree with that of other gamma-ray detected star-forming galaxies in ACK12, whereas the mean photon index of LAT-detected FSRQs is -2.46 (Abdo et al. 2010b). Therefore, based on the gamma-ray spectrum and light curve, we conclude that the gamma-ray excess is dominantly contributed by NGC 2146, although a small contribution by CRATES J061758+781552

can not be formally excluded.

2.3. M51, NGC 1365, Arp 220 and M83

Four more sources with significant gamma-ray excesses were found in the vicinity of M51 (TS=29.9), NGC 1365 (TS=44.4), Arp 220 (TS=52.2) and M83 (59.1); however, the best-fit positions are all far from the core of the corresponding galaxies, i.e., the angular separation is larger than r_{95} , c.f., Table 1. We therefore explored possible candidate sources for those gamma-ray excess within r_{95} .

M51. The gamma-ray excess next to M51 likely comes from SDSS J13261+4754, with an angular separation of 0.13° between them, which is smaller than r_{95} .

NGC 1365. The gamma-ray excess is likely associated with PKS 0335–364, a strong radio quasar, with an angular separation of 0.07° between them.

Arp 220. Both CRATES J153246+234400 (a FSRQ) and SDSS J15323+2333 (a Seyfert 2 galaxy at $z=0.047$) may contribute to the gamma-ray excess since their angular separations are just 0.16° and 0.14° , respectively. We further constructed an annual light curve of the gamma-ray emission and found a significant variability (a factor of 4 between the highest and lowest annual flux) in this gamma-ray excess. We therefore conclude that the gamma-ray emission more likely comes from the FSRQ CRATES J153246+234400.

M83. The possible source contributes to the gamma-ray excess is MS 13326-2935, a blazar in Veron-Cetty catalogue (also named 2E 3100), which is 0.04° away from the best-fit position. The result is consistent with Lenain & Walter (2011), where a gamma-ray excess compatible with 2E 3100 with TS=30.1 is found.

The maximum likelihood analysis results of all the 7 starburst galaxies in this study are shown in Table 2. We also perform additional maximum likelihood analysis in the energy range from 100 MeV to 100 GeV, such that our results can readily be compared with upper limits reported in ACK12. All upper limits from this study are smaller than the corresponding ones reported in ACK12, the latter using a smaller data set. Note that, for the four star-forming galaxies, M51, NGC 1365, Arp 220 and M83, we calculated upper limits of their gamma-ray flux by adding a point source at the best-fit position to build a new source background model.

3. INTERPRETATION AND IMPLICATION OF THE GAMMA-RAY EMISSION FROM NGC 2146

3.1. Interpretation of the gamma-ray emission from NGC 2146

The gamma-ray emission of starburst galaxies could, in principle, be produced by Bremsstrahlung and inverse-Compton emission of the primary or secondary electrons, as well as the pionic decay emission resulted from CR interactions. Detailed calculations have shown that the pionic decay gamma-rays dominate the emission above 100 MeV for starburst galaxies (e.g. Domingo-Santamaría & Torres (2005); Rephaeli et al. (2010)), although leptonic emission is expected to become increasingly important at lower energies.

The total injected CR power in the galaxies scales with the SN rate as SNRs are the primary CR accelerators. Following Thompson et al. (2007), we assume that the supernova rate is a constant fraction, Γ_{SN} , of the star-formation rate (\dot{M}_*) and a fraction of $5\eta_{0.05}\%$ of its kinetic energy E_{SN} is supplied to relativistic protons, thus the total CR power is $L_{\text{CR}} = \Gamma_{\text{SN}}\dot{M}_*\eta E_{\text{SN}}$. Assuming that the star-formation rate is related to the total infrared (IR) luminosity in 8-1000 μm by

$L_{8-1000\mu\text{m}} = \epsilon \dot{M}_* c^2$, the total CR power is (see also Eq. 5 in Thompson et al. (2007))

$$L_{\text{CR}} = 4.6 \times 10^{-4} L_{8-1000\mu\text{m}} E_{51} \eta_{0.05} \beta_{17}, \quad (1)$$

where $E_{51} = E_{\text{SN}}/10^{51}\text{ergs}$ and $\beta_{17} \equiv (\Gamma_{\text{SN}}/\epsilon)/17M_{\odot}^{-1}$, which depends weakly on the initial mass function (Thompson et al. 2007). In the proton calorimeter limit, i.e. all the proton energy is lost into secondary pions, the gamma-ray luminosity is directly related to the CR power by $L_{\gamma}(> 0.1\text{GeV}) \simeq \frac{1}{3} L_{\text{CR}}$, where $\frac{1}{3}$ comes from the fact that only $\frac{1}{3}$ of the proton energy lost goes into neutral pions and we have assumed that the energy in gamma-rays below 0.1 GeV is negligible. Then the ratio between the total gamma-ray luminosity and the total infrared luminosity in the calorimeter limit is

$$\xi \equiv \frac{L_{\gamma}(> 0.1\text{GeV})}{L_{8-1000\mu\text{m}}} = 1.5 \times 10^{-4} E_{51} \eta_{0.05} \beta_{17}, \quad (2)$$

as has been predicted in Thompson et al. (2007). We compare the ratio between the observed gamma-ray luminosity and total infrared luminosity of NGC 2146 with this limit ratio in Fig.3 (together with other LAT detected galaxies) and find that NGC 2146 lies close to this calorimeter limit. Thus, we suggest that NGC 2146 is probably a "proton calorimeter".

The proton calorimetry of NGC 2146 can be understood by comparing the collisional energy loss time of CR protons and the escape time (Loeb & Waxman 2006; Thompson et al. 2007). For a gas density of $n \sim 10\text{cm}^{-3}$ in the starburst region of NGC 2146 (Greve et al. 2006), the collisional energy loss time of CR protons is

$$t_{pp} = (0.5n\sigma_{pp}c)^{-1} = 5 \times 10^6 \text{yr} \left(\frac{n}{10\text{cm}^{-3}} \right)^{-1}, \quad (3)$$

where the factor 0.5 is inelasticity, and σ_{pp} is the inelastic nuclear collision cross section. If t_{pp} is less than the escape time, then system is a proton calorimeter. CR protons can escape by advection in galactic winds¹, with a timescale

$$t_{ad} = h/v = 4 \times 10^6 \text{yr} \left(\frac{h}{1\text{kpc}} \right) \left(\frac{v}{250\text{kms}^{-1}} \right)^{-1}, \quad (4)$$

where $h \simeq 1\text{kpc}$ is the size of the starburst region (Greve et al. 2006) and $v = 250 - 300\text{kms}^{-1}$ is the velocity of the galactic wind in NGC 2146 (Kreckel et al. 2014). Comparing Eqs.(3)-(4), we expect that CR protons in the starburst region of NGC 2146 should lose a large fraction of their energy before escape, in agreement with the above inferred large calorimetry fraction.

3.2. Correlation between the γ -ray luminosity and total IR luminosity

It has been proposed that there is a connection between galaxy star-formation rates and gamma-ray luminosities, motivated by the connections between the star-formation rate, SN rate and cosmic ray power (e.g. Pavlidou & Fields (2002); Torres (2004); Thompson et al. (2007); Stecker (2007); Persic & Rephaeli (2010); Lacki et al. (2011)). Thompson et al. (2007) first predicted a far infrared (FIR)–gamma-ray correlation in the calorimetric limit for densest starbursts. ACK12 found a quasi-linear scaling relation between gamma-ray luminosity and the total IR luminosity for quiescent galaxies in the Local group and nearby starburst

galaxies. We now examine whether NGC 2146 follows this relation. Different from ACK12, we exclude two starbursting Seyfert 2 galaxies NGC 1068 and NGC 4945 in the fit in order to have a sample consist purely of star-forming and starburst galaxies. Fig. 4 shows their gamma-ray luminosities and total IR luminosities(8-1000 μm) of this sample. The total IR(8-1000 μm) luminosities are provided by Gao & Solomon (2004) and the gamma-ray luminosities are from Ackermann et al. (2012). We fit the data with a simple power-law and find the relation

$$\frac{L_{0.1-100\text{GeV}}}{\text{erg s}^{-1}} = 10^{39.772 \pm 0.085} \left(\frac{L_{8-1000\mu\text{m}}}{10^{44}\text{erg s}^{-1}} \right)^{1.285 \pm 0.058}, \quad (5)$$

with a Pearson correlation coefficient being $r = 0.983$ and null hypothesis probability less than 10^{-4} , which indicates a tight positive correlation. The scaling indices between the gamma-ray luminosity and total IR luminosity for this sample is consistent within uncertainties with that obtained in previous works (Abdo et al. 2010a; Ackermann et al. 2012). With NGC 2146, the highest IR luminosity galaxy in this sample, the correlation now extends up to a total IR luminosity of $10^{11}L_{\odot}$, strengthening the connection between massive star formation and gamma-ray emission of star-forming galaxies.

3.3. Prediction for very high emission from NGC 2146

Very high energy (VHE) gamma-ray emission has been detected from nearby starburst galaxies M82 and NGC 253 by VERITAS and HESS, respectively (Acciari et al. 2009; Acero et al. 2009). Using the GeV flux and the spectrum of NGC 2146, we can estimate the VHE flux assuming a simple power-law extrapolation. As can be seen from Fig.2 (left panel), the predicted energy flux is $E^2 dN/dE \simeq 10^{-13}\text{TeVcm}^{-2}\text{s}^{-1}(E/1\text{TeV})^{-0.1}$ at TeV energies, which is close to the detection sensitivity of VERITAS and should be detectable by future instruments such as CTA, LHAASO and etc. Note that at a distance of 15.2 Mpc, the absorption by extragalactic background light is unimportant for TeV photons.

Proton-proton collisions in starbursts not only produce neutral pions, but also produce charged pions, which then decay and produce neutrinos. Loeb & Waxman (2006) argued that supernova remnants in starburst galaxies accelerate CR protons and produce high-energy neutrinos. Loeb & Waxman (2006), Thompson et al. (2007) and Lacki et al. (2011) further made an explicit connection between the expected diffuse gamma-ray background and the diffuse high-energy neutrino background from starbursts since pion production links the two directly. Recently, the IceCube Collaboration reported 37 events ranging from 60 TeV to 3 PeV within three years of operation, correspond to a 5.7σ excess over the background atmospheric neutrinos and muons(Aartsen et al. 2014). One attractive scenario for this excess is that they are produced by cosmic rays in starburst galaxies(Murase et al. 2013; Liu et al. 2014). But whether neutrinos in starburst galaxies can extend to sub-PeV/PeV energies is uncertain, given that normal supernova remnants are usually believed to accelerate protons only to $\lesssim 1\text{PeV}$. It was suggested that hypernova remnants in starburst galaxies, by virtue of their fast ejecta, are able to accelerate protons to $\gg \text{PeV}$ (Wang et al. 2007) and produce sub-PeV/PeV neutrinos (Liu et al. 2014). Future observations of VHE gamma-ray emission of starburst galaxies extending to $\gtrsim 100\text{TeV}$ would be able to pin down the starburst origin of the sub-PeV/PeV neutrinos.

4. SUMMARY

¹ CRs can also escape via diffusion. However, since the diffusion coefficient in starburst galaxies is not known, this timescale is uncertain.

By searching for high-energy gamma-ray emission from the 7 best candidate galaxies for LAT detection beyond the Local group (ACK12), we found significant high-energy gamma-ray emission above 100 MeV from a source spatially coincident with NGC 2146, the nearest LIRG galaxy. The significance of the detection is about 5.5σ . This is the first time that a LIRG galaxy has been detected by Fermi/LAT. The high gamma-ray luminosity suggests that cosmic ray protons in NGC 2146 convert most of their energy into secondary pions, so NGC 2146 is a proton calorimeter. It is also found that NGC 2146 extends the quasi-linear scaling relation between the gamma-ray luminosities and total IR luminosities of star-forming galaxies to a higher luminosity, thus strengthening the connection between massive star formation and gamma-ray emission of star-forming galaxies.

We thank J. Q. Sun, J. F. Wang, K. Bechtol, C. D. Dermer for helpful discussion. This work has made use of data and software provided by the Fermi Science Support Center. This work also made use of NASA's Astrophysics Data System, and the NASA/IPAC Extragalactic Database (NED) which is operated by the Jet Propulsion Laboratory, California Institute of Technology, under contract with NASA. This work is supported by the 973 program under grant 2014CB845800, the NSFC under grants 11273016 and 11033002, and the Excellent Youth Foundation of Jiangsu Province (BK2012011). PHT is supported by the Ministry of Science and Technology of the Republic of China (Taiwan) through grant 101-2112-M-007-022-MY3.

REFERENCES

- Aartsen, M. G., Ackermann, M., Adams, J., et al. 2014, arXiv:1405.5303
- Abdo, A. A., Ackermann, M., Ajello, M., et al. 2010a, *ApJ*, 709, L152
- Abdo, A. A., Ackermann, M., Ajello, M., et al. 2010b, *ApJ*, 710, 1271
- Abdo, A. A., Ackermann, M., Ajello, M., et al. 2010c, *A&A*, 523, L2
- Acciari, V. A., 2009, *Nature*, 462, 770
- Acero, F. et al. 2009, *Science*, 326, 1080
- Ackermann, M., Ajello, M., Allafort, A., et al. 2012, *ApJ*, 755, 164 (ACK12)
- Caccianiga, A., Maccacaro, T., Wolter, A., Della Ceca, R., & Gioia, I. M. 2000, *A&AS*, 144, 247
- Domingo-Santamaría, E., & Torres, D. F. 2005, *A&A*, 444, 403
- Gao, Y., & Solomon, P. M. 2004, *ApJ*, 606, 271
- Greve, A., Neininger, N., Sievers, A., & Tarchi, A. 2006, *A&A*, 459, 441
- Ginzburg, V. L., & Syrovatskii, S. I. 1964, *The Origin of Cosmic Rays*, New York: Macmillan, 1964,
- Hayashida, M. et al. 2013, 779, 131
- Healey, S. E., Romani, R. W., Taylor, G. B., et al. 2007, *ApJS*, 171, 61
- Healey, S. E., Romani, R. W., Cotter, G., et al. 2008, *ApJS*, 175, 97
- Kreckel, K., Armus, L., Groves, B., et al. 2014, *ApJ*, 790, 26
- Lacki, B. C., Thompson, T. A., & Quataert, E. 2010, *ApJ*, 717, 1
- Lacki, B. C., Thompson, T. A., Quataert, E., Loeb, A., & Waxman, E. 2011, *ApJ*, 734, 107
- Lacki, B. C., & Thompson, T. A. 2013, *ApJ*, 762, 29
- Lenain, J.-P., & Walter, R. 2011, *A&A*, 535, A19
- Liu, R.-Y., Wang, X.-Y., Inoue, S., Crocker, R., & Aharonian, F. 2014, *Phys. Rev. D*, 89, 083004
- Loeb, A., & Waxman, E. 2006, *JCAP*, 5, 3
- Mattox, J. R., Bertsch, D. L., Chiang, J., et al. 1996, *ApJ*, 461, 396
- Murase, K., Ahlers, M., & Lacki, B. C. 2013, *Phys. Rev. D*, 88, 121301
- Nolan, P. L., Abdo, A. A., Ackermann, M., et al. 2012, *VizieR Online Data Catalog*, 219, 90031
- Pavlidou, V., & Fields, B. D. 2002, *ApJ*, 575, L5
- Persic, M., & Rephaeli, Y. 2010, *MNRAS*, 403, 1569
- Rephaeli, Y., Arieli, Y., & Persic, M. 2010, *MNRAS*, 401, 473
- Sanders, D. B., & Mirabel, I. F. 1996, *ARA&A*, 34, 749
- Stecker, F. W. 2007, *Astroparticle Physics*, 26, 398
- Thompson, T. A., Quataert, E., & Waxman, E. 2007, *ApJ*, 654, 219
- Torres, D. F. 2004, *ApJ*, 617, 966
- Véron-Cetty, M.-P., & Véron, P. 2010, *A&A*, 518, A10
- Wang, X.-Y., Razzaque, S., Mészáros, P., & Dai, Z.-G. 2007, *Phys. Rev. D*, 76, 083009

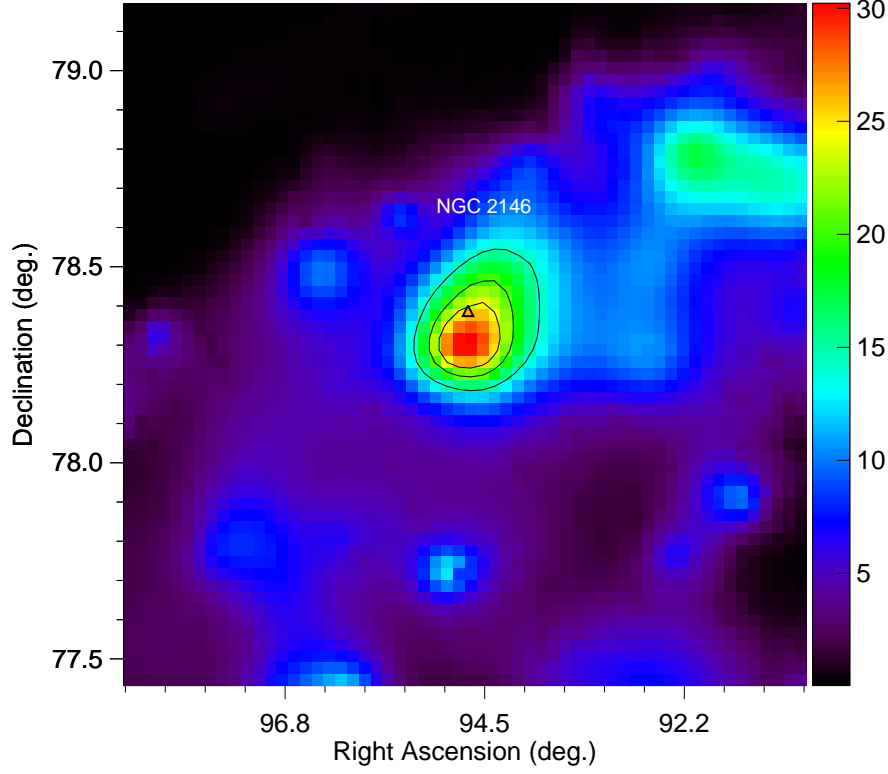


FIG. 1.— Test statistic map obtained from photons above 200 MeV showing the celestial region (1.8° by 1.8° , a pixel with 0.03×0.03 squared-degrees) around NGC 2146. The black empty triangle indicates the optical position of NGC 2146; black lines show the 1σ , 2σ , and 3σ confidence level contours on the position of the observed gamma-ray excess. The color scale indicates the point-source TS value at each location on the sky.

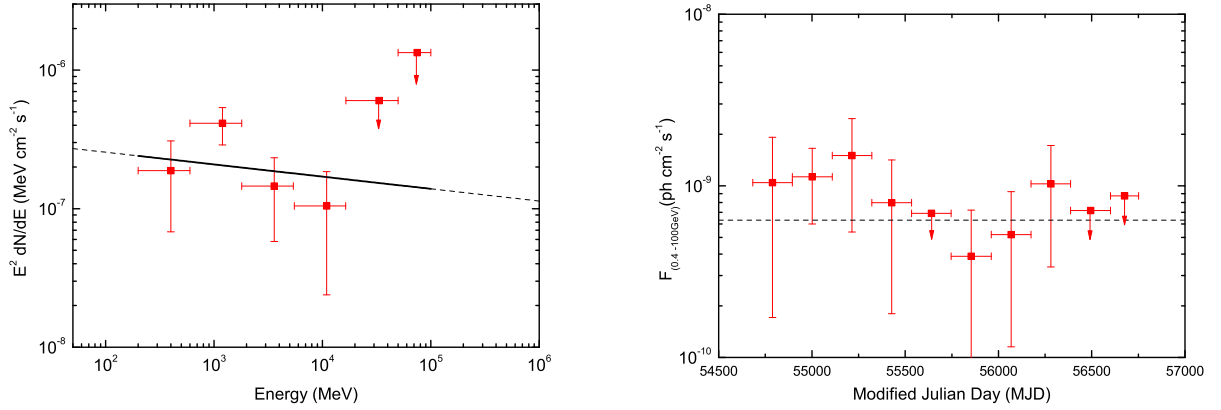


FIG. 2.— Left: Spectral energy distribution for NGC 2146 obtained in the analysis of the 68 months of data as described in the text. The black solid line represents the best-fit power law in the range of 0.2–100 GeVs shown in Table 1. Right: Gamma-ray (>400 MeV) light curve for NGC 2146 obtained in the analysis of the 68 months of data. The 68 month observation period was divided into 10 time intervals for analysis. The dashed black line shows the maximum likelihood flux level obtained for the full 68 months observation period. One- σ errors are shown for energy bins with $TS > 1$ and 95% confidence-level upper limits are shown otherwise.

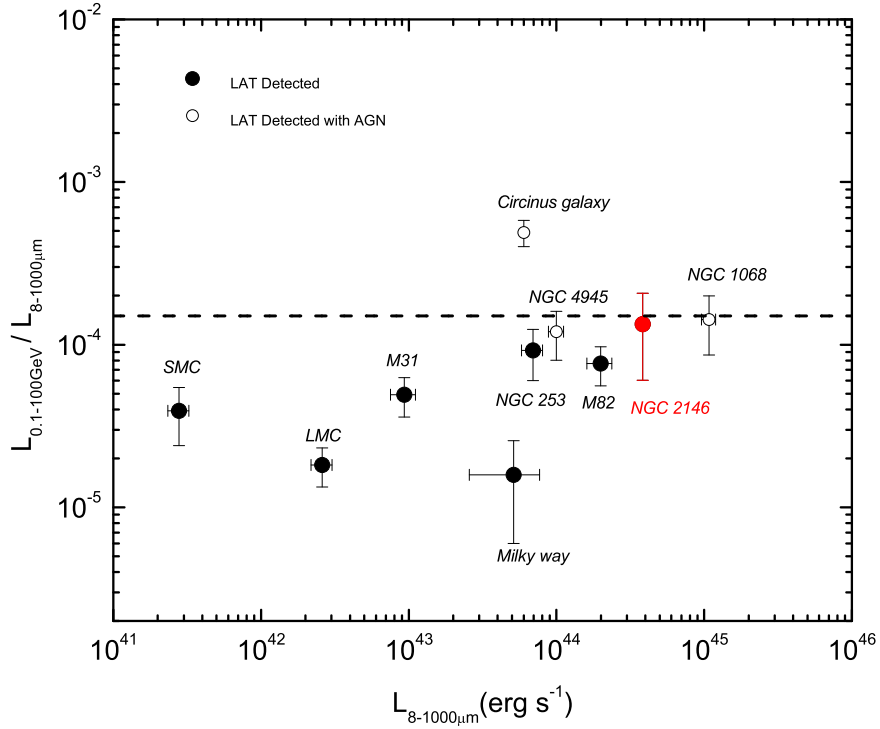


FIG. 3.— The ratio between the gamma-ray luminosities and total IR luminosities for LAT-detected star-forming galaxies and Seyferts. The dotted horizontal line corresponds to the proton calorimetric limit (see the text for details). The data for the Circinus galaxy, which is an anomalously gamma-ray bright Seyfert galaxy, is taken from Hayashida et al. (2013). For other galaxies, the values of the total IR(8-1000 μ m) luminosities are taken from Gao & Solomon (2004) and the gamma-ray luminosities (except for NGC 2146) are taken from Ackermann et al. (2012)

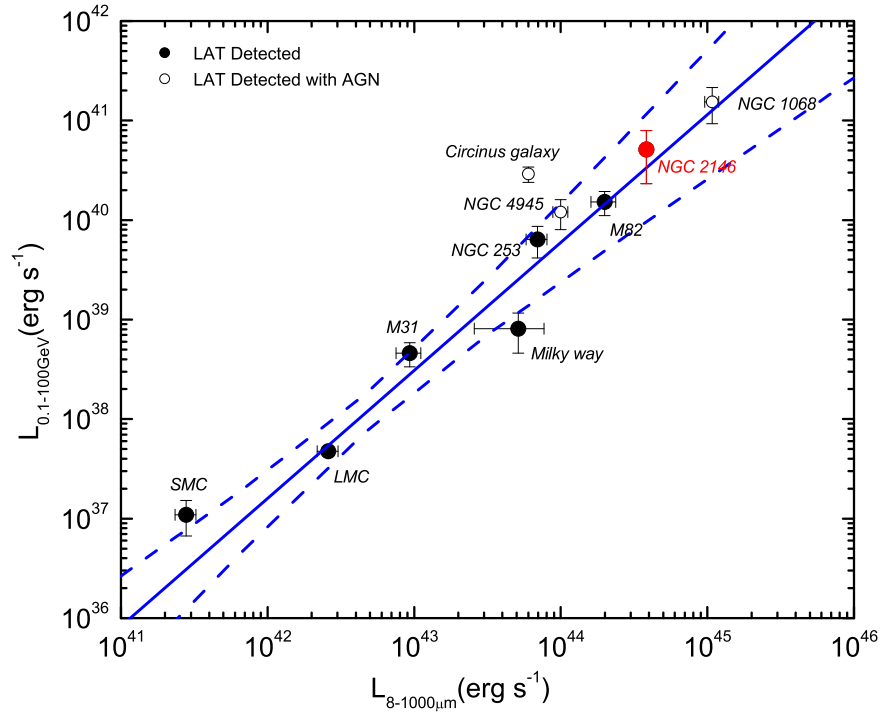


FIG. 4.— The relation between the gamma-ray luminosity (0.1-100 GeV) and total IR luminosity (8-1000 μ m) for star-forming galaxies. The red solid line is the best fit, while the blue and green dashed lines represent the upper and lower limits, respectively, at 95% confidence. Note that two starbursting Seyfert galaxies (NGC 1068 and NGC 4945) and the Circinus galaxy are excluded in the fit in order to have a sample consist purely of star-forming and starburst galaxies.

TABLE 1

BEST-FIT POSITION AND ANALYSIS RESULTS OF THE FIVE NEW SIGNIFICANTLY DETECTED GAMMA-RAY SOURCES IN THE VICINITY OF THE GALAXIES.

Galaxy	R.A. & Decl. ^a (deg)	r_{95} ^b (deg)	δAngle^c (deg)	$F(0.2-100\text{GeV})$ (10^{-9} ph cm $^{-2}$ s $^{-1}$)	Γ	TS	Association ^d
NGC 2146	(94.55, 78.30)	0.11	0.06	1.1 ± 0.5	2.1 ± 0.2	30.8	(1)
M51	(201.66, 47.81)	0.21	0.80	2.8 ± 0.8	2.8 ± 0.2	29.9	(2)
NGC 1365	(54.17, -36.33)	0.30	0.65	3.2 ± 0.7	2.6 ± 0.2	44.4	(3)
Arp 220	(233.24, 23.58)	0.20	0.46	3.2 ± 0.7	2.3 ± 0.1	52.2	(4)
M83	(203.84, -29.82)	0.07	0.36	1.2 ± 0.5	1.8 ± 0.2	58.1	(5)

^aBest-fit position of gamma-ray excess^bThe 95% containment error circle radius around the best-fit position^cThe angular separation between the best-fit position and the position of the core of the galaxy^dThe most likely associated source, as shown in Sects. 2.2 and 2.3: (1) NGC 2146; (2) SDSS J13261+4754; (3) PKS 0335-364; (4) CRATES J153246+234400; (5) MS 13326-2935(2E 3100).

TABLE 2

MAXIMUM LIKELIHOOD ANALYSIS RESULTS AT THE CORE OF THE STARBURST GALAXIES.

Galaxy	D ^a (Mpc)	$F(0.2-100\text{GeV})$ (10^{-9} ph cm $^{-2}$ s $^{-1}$)	Γ	$L_{0.2-100\text{GeV}}$ (10^{40} erg s $^{-1}$)	TS	$F(0.1-100\text{GeV})$ (10^{-9} ph cm $^{-2}$ s $^{-1}$)
M83 ^b	3.7	<1.2	2.2	<0.3	...	<2.3
M101	6.4	<0.6	2.2	<0.4	...	<1.1
M51 ^b	9.6	<1.2	2.2	<1.8	...	<2.9
NGC 2146	15.2	1.1 ± 0.6	2.1 ± 0.2	4.0 ± 2.1	26.4	1.4 ± 1.0
NGC 1365 ^b	20.8	<0.8	2.2	<5.7	...	<1.7
NGC 3690	41.1	<0.9	2.2	<23.5	...	<1.6
Arp 220 ^b	74.7	<1.5	2.2	<137.1	...	<3.5

^aDistances are taken from Ackermann et al. (2012).^bAn additional point source at the best-fit position was added in the source model as discussed in text.